Article:
Adams, K.D. and Rhodes, E.J. (2019) Late Holocene paleohydrology of Walker Lake and the Carson Sink in the western Great Basin, Nevada, USA. Quaternary Research, 92 (1). pp. 165-182. ISSN: 0033-5894

https://doi.org/10.1017/qua.2018.151

Late Holocene paleohydrology of Walker Lake and the Carson Sink in the western Great Basin, Nevada, USA

Kenneth D. Adams*
Desert Research Institute
2215 Raggio Parkway
Reno, NV 89512
USA
(775) 673-7345
kadams@dri.edu

Edward J. Rhodes
Department of Geography
University of Sheffield,
Sheffield, S10 2TN
United Kingdom

*Corresponding author

ABSTRACT

The late Holocene histories of Walker Lake and the Carson Sink were reconstructed by synthesizing existing data in both basins along with new age constraints from key sites, supplemented with paleohydrologic modeling. The repeated diversions of the Walker River to the Carson Sink and then back to Walker Lake caused Walker Lake-level fluctuations spanning 50 $\pm$ m. Low lake levels at about 1000, 750, and 300 cal yr BP are time correlative to the ages of fluvial deposits along the Walker River paleochannel, when flow was directed toward the Carson Sink. The timing and duration of large lakes in the Carson Sink was further refined using moisture-sensitive tree ring chronologies. The largest lakes required a 4 – 5-fold increase in discharge spanning decades. Addition of Walker River flow to the Carson Sink by itself is inadequate to account for the required discharge. Instead, increases in the runoff coefficient and larger areas of the drainage basin contributing surface runoff may explain the enhanced discharge required to create these large lakes.

Keywords: Lake Lahontan, Walker Lake, Carson Sink, Holocene, paleohydrologic modeling

INTRODUCTION

Paleohydrologic records from Great Basin pluvial lakes provide a rich source of information enhancing understanding of the character, magnitudes, and rates of past climatic changes (e.g., Smith and Street-Perrot, 1983; Benson and Thompson, 1987a; Morrison, 1991; Benson, 2004; Reheis et al., 2014). Although most of these lakes had

45 evaporated by the end of the Pleistocene, a few small lakes remained that were fed by
46 perennial rivers sourced in high mountains. These extant lakes have continued to record
47 climatic perturbations through the Holocene by altering their depths, surface areas, and
48 volumes according to the water balance of their watersheds.

49 This paper focuses on the late Holocene histories of Walker Lake and the Carson Sink
50 in western Nevada. These lakes were integrated when Lake Lahontan was at high levels
51 during the late Pleistocene but separated during early Holocene desiccation. Throughout
52 the Holocene, however, their histories remained linked by the unusual behavior of the
53 Walker River, which periodically switched course from one terminal basin to the other
54 (Russell, 1885; Benson and Thompson, 1987a, b; Benson et al., 1991; King, 1993, 1996;
55 Adams, 2003, 2007). Lake-level changes in these basins therefore not only reflect climate
56 changes but also the wandering behavior of the Walker River. Here, new data and
57 interpretations on Holocene lake-level fluctuations at Carson Sink and Walker Lake
58 augment records developed in Benson et al. (1991), Adams (2003, 2007), Bell et al.
59 (2010), and Bell and House (2010). Together with new stratigraphy indicating timing of
60 river diversions, these data refine the climatic and physiographic controls on lake-level
61 history.

62 The lake-level and river-flow records are then analyzed, with respect to the historical
63 hydrology of these systems, in terms of the timing, rates, magnitudes, and areas of
64 hydrologic change during the late Holocene. In particular, the moisture-sensitive gridded
65 tree ring database contained within the Living Blended Drought Atlas (Cook et al., 2010)
66 assists in the characterization of the duration, magnitude, and geographical extent of wet
67 and dry periods over the last 2000 years. This information enables refinement of

68 shoreline ages, and, by simple paleohydrologic modeling, estimates of the rates and
69 magnitudes of past lake-level changes.
70
71 **REGIONAL SETTING AND HYDROLOGY**
72 The Carson Sink and Walker Lake represent adjacent subbasins of the pluvial Lake
73 Lahontan system in western Nevada. These lakes were part of a single waterbody only
74 when levels were above about 1310 m (King, 1993), which is close to the late Pleistocene
75 highstand elevation (~1332 m) in the area (Adams et al., 1999). Currently, Walker Lake
76 is fed by a drainage basin extending over about 10,200 km^2, with the West Walker and
77 East Walker rivers being the major tributaries that join together to form the Walker River
78 at the south end of Mason Valley before flowing north and then turning south toward
79 Walker Lake (Figs. 1 and 2).
80 Cumulative mean annual discharge for both branches of the Walker River during the
81 historical period (1926 – 2017) is about 0.38 km^3/yr, with flows during the wettest years
82 ranging up to about 1 km^3/yr (Table 1). According to the Parameter-elevation
83 Regressions on Independent Slopes Model (PRISM) (Daly et al., 2008), the highest parts
84 of the drainage basin along the Sierran crest receives from 100 to 170 cm/yr of mean
85 annual precipitation, most of which accumulates in the winter as snow (Fig. 1). In
86 contrast, precipitation at Walker Lake ranges from about 12 to 20 cm/yr (Fig. 1) (Daly et
87 al., 2008).
88 Harding (1965) and Milne (1987) estimated that the mean annual lake evaporation
89 rate for Walker Lake is about 125 cm/yr. Allander et al. (2009) measured evaporation
90 from a floating platform in Walker Lake for a two-year period and determined that the

91 actual annual lake evaporation rate was about 152 cm/yr. Allander et al. (2009) attributed
92 the difference between these two values to be due to previously unaccounted groundwater
93 inflow, based on a water budget approach.
94 At its historical highstand in 1868, Walker Lake reached an elevation of about 1252
95 m, had a surface area of about 300 km^2, and a volume of about 13 km^3 (Adams, 2007;
96 Lopes and Smith, 2007). Because of drought and upstream water diversions and
97 consumption, the lake-surface elevation had dropped to about 1191 m at the start of the
98 2017 water year, corresponding to a surface area of about 109 km^2 and volume of about
99 1.2 km^3. Due to the unusually deep snowpack of the 2016-17 winter in its headwaters,
100 runoff down the Walker River had raised the level of the lake by just over 3 meters by the
101 start of the 2018 water year.
102 The Carson and Humboldt sinks (herein shortened to the Carson Sink) occupy the
103 lowest part of a drainage basin that encompasses about 54,000 km^2 and is primarily fed
104 by the Carson River from the west and the much larger Humboldt River drainage basin
105 from the east (Figs. 1 and 2). The Carson River also derives most of its flow from near
106 the Sierran crest where precipitation is about 100 to 140 cm/yr (Daly et al., 2008). As the
107 Carson River enters the basin near Fallon, NV, it splits into a series of distributaries that
108 alternately direct flow either to the Carson Sink (aka North Carson Lake), or east to
109 Stillwater Marsh, or southeast to Carson Lake (Fig. 2). Since the mid-19th century most of
110 the flow has been directed toward Carson Lake (Morrison, 1964), which has a surface
111 area of ~ 150 km^2 and volume of ~ 0.4 km^3 when it is overflowing north through the
112 Stillwater Slough to Stillwater Marsh and then into the Carson Sink (Adams, 2003). The

historic highstand in the Carson Sink occurred in 1862 when lake level reached 1185.7 m, corresponding to an area of 1300 km^2 and volume of 5.7 km^3 (Fig. 2).

Much of the flow in the Humboldt River is derived from the Ruby Mountains where precipitation ranges from about 80 to 110 cm/yr, also mostly snow, although significant volumes of water are probably occasionally derived from the Santa Rosa, Independence, Jarbidge, and Toiyabe ranges (Fig. 1). The Humboldt River typically terminates in the Humboldt Sink (Fig. 2), which is separated from the rest of the Carson Sink by a valley-spanning beach ridge complex known as the Humboldt Bar (Russell, 1885). A narrow channel cut through the lowest part of the Humboldt Bar indicates occasional flow from the Humboldt Sink south to the Carson Sink. During the mid-1980s highstand in the Carson Sink (1183 m; 890 km^2; 2.5 km^3) (Fig. 2), almost twice the volume of water came down the Humboldt River as did from the Carson River even though their average annual flows are very similar (Table 1).

PREVIOUS WORK

Morrison (1964) documented the existence of low elevation shorelines (< 1204 m) rimming the Carson Sink that he grouped as part of the late Holocene Fallon Formation (later renamed the Fallon Alloformation; Morrison, 1991). Davis (1978) identified the Turupah Flat tephra (< 2 ka) within the Salt Wells beach barrier (~1202 m) and Adams (2003) dated detrital charcoal from 5 cm beneath the tephra to 660 – 910 cal yr BP. A slightly lower beach (~1198 m) was dated to 1310 -1520 cal yr BP (Adams, 2003).

Bell et al. (2010) and Bell and House (2010) mapped the Lahontan Mountains and Grimes Point quadrangles, respectively, and reported 25 new radiocarbon ages bearing on

136 the late Pleistocene and Holocene history of the Carson Sink. In particular, they
137 documented ages and elevations of key outcrops and landforms consistent with results of
138 previous studies but add detail to the record of late Holocene lake-level fluctuations.
139 In the Walker Lake subbasin, Benson (1978) used the ages and elevations of tufa
140 samples to construct a Holocene lake-level curve, which was updated by Benson and
141 Thompson (1987a, b), Benson (1988), and Benson et al. (1991) with the addition of lake-
142 level proxies from deep-water cores. Large-scale lake-level drops at about 2 ka and 1 ka
143 were attributed to temporary diversion of the Walker River out of the basin (Benson et
144 al., 1991). Bradbury et al. (1989) added to this history using biological proxies from the
145 cores. The late Holocene tufa ages of Newton and Grossman (1988) are largely in
146 agreement with the results of Bradbury et al. (1989) and Benson et al. (1991). Yuan et al.
147 (2004, 2006) collected additional cores and used fluctuations in several proxies to infer
148 hydrologic fluctuations over the last 2700 years.
149 Adams (2007) used radiocarbon ages from terrestrial plant material and charcoal
150 collected from diverse sedimentary environments including fluvial, deltaic, beach, and
151 offshore settings to refine the late Holocene curve for Walker Lake. The revised curve
152 confirmed several large-scale fluctuations over the last few thousand years (Adams,
153 2007). Because the study focused on stratigraphic sections and not shorelines, however,
154 the maximum elevations of Holocene highstands could only be estimated. Subsequent
155 geologic mapping along the lower Walker River and at Walker Lake by House and
156 Adams (2009, 2010) identified the upper limit of late Holocene beach deposits at about
157 1262 m.

158 Hatchett et al. (2015) used a coupled water balance and lake evaporation model along
159 with the Walker Lake-level curve of Adams (2007) to simulate the climatic conditions
160 that led to two lowstands separated by a minor highstand during the Medieval Climate
161 Anomaly (MCA). This sequence of drought-deluge-drought generally fits the pattern of
162 western U.S. hydroclimate during the MCA originally defined by Stine (1994), which
163 was in part based on the death ages of trees found within the West Walker River channel
164 near its headwaters. The timing of this sequence was refined by Cook et al. (2010).
165 Hatchett et al. (2015), however, did not consider the effect of the wandering behavior of
166 the Walker River on Walker Lake levels, which means that the lake-level fluctuations
167 that they were modeling may have had additional non-climate controls.
168 Multiple studies (e.g., Davis, 1982; King, 1993, 1996; Benson and Thompson,
169 1987a,b; Benson et al., 1991; Adams, 2007) concluded that during the Holocene the
170 Walker River was occasionally diverted from the Walker Lake subbasin to become a
171 tributary of the Carson River and Carson Sink (Fig. 2), but the timing of these diversions
172 (and returns) was unclear. During such diversions, the Carson Sink received substantial
173 additional water and Walker Lake was deprived of its only major water source.
174 King (1993, 1996) concluded that diversions of the Walker River through Adrian
175 Valley were as recent as within the last few hundred years, based on the ages of
176 Anodonta shells (300 ± 60 ^{14}C yr BP) found along the paleochannel. S.J. Caskey (pers.
177 comm., 2004) determined a similar age (330 ± 60 ^{14}C yr BP) from other Anodonta shells
178 along the same reach.
179 The sum of evidence from multiple studies indicates that Walker Lake has undergone
180 multiple large-scale lake-level fluctuations during the late Holocene. Whether this was

strictly due to climate change or to the occasional diversion of the Walker River out of and back into the basin is one of the topics addressed in this paper.

METHODS

This synthesis compiles existing radiocarbon data from a number of published sources that bear on the Holocene histories of Walker Lake and the Carson Sink, as well as presents new radiocarbon and infrared stimulated luminescence (IRSL) ages for key outcrops and landforms. All radiocarbon ages have been calibrated with the Calib 7.1 program using the IntCal13 calibration curve (Reimer et al., 2013) and are reported in radiocarbon years before present (^{14}C yr BP) and calibrated years before present (cal yr BP). The reservoir effect associated with lakes in the Carson Sink and the Walker River are unknown so radiocarbon ages of mollusk shells from these locales are not corrected, but are assumed to represent maximum ages. Luminescence ages have been corrected to reflect calibrated years before present (1950 AD).

Luminescence samples were collected from six hand excavated pits on a suite of beach ridges near the north end of Walker Lake. Duplicate samples were collected by pounding a steel pipe horizontally into the vertical wall of each sample pit and then excavating the pipe and capping the ends with light-tight material. An attempt was made to sample parts of the exposures with visible bedding, in order to minimize the mixing effects of bioturbation. In situ gamma spectrometer measurements were collected from the same holes where the sediment was collected to determine dose rate, in addition to a bulk sample surrounding each sample site for laboratory radiation measurements. All samples were prepared and processed at the University of California, Los Angeles

luminescence laboratory using the single grain K-feldspar post IR IRSL protocol outlined in Rhodes (2015). More details on this methodology are found in the supplementary data.

Calibrated radiocarbon ages from the late Holocene typically have a 2-sigma error range of several hundred years, which makes it difficult to assess rates of hydrologic change that typically occur over shorter periods (e.g., Adams et al., 2015). For selected radiocarbon samples from the Carson Sink, the moisture-sensitive tree ring chronologies contained within the Living Blended Drought Atlas (LBDA) of Cook et al. (2010) were used to refine the timing and duration of lake highstands associated with particularly wet periods. The LBDA provides a year by year view of the spatial-temporal distribution of drought areas and relatively wet regions across North America that extends back to the year 0 AD (Cook et al., 2010). This information can be viewed in the form of maps or by examining the annual time series of Palmer Drought Severity Index (PDSI) values for the summer months (JJA) at a particular grid node within the LBDA (Fig. 1). Although there are higher numbers of chronologies for younger time periods, more than 15 chronologies contribute to PDSI values for the grid nodes in the Humboldt, Carson, and Walker basins that begin in the time period 500 – 1500 AD and three that extend to the year 0 AD (Figure 1, inset).

Assuming that large lakes in the Carson Sink reflect extended periods of above average precipitation within its headwaters, the LBDA time series can guide estimates of timing, duration, and magnitude of specific wet periods encompassed by the imprecise radiocarbon ages associated with high lake levels. Here we assume the beginning of the lake-level rise coincides with the beginning of the wet period as indicated by positive PDSI values, and that the maximum lake level is attained the year before PDSI values

become negative. We estimated the number of years it took for the lakes to desiccate by applying the modern evaporation rate (~ 130 cm/yr) to the depths of the lakes, but recognize that this is a minimum duration estimate.

The elevations of dating samples and landforms measured for this study were surveyed with either a total station referenced to local benchmarks, high precision GPS instruments, or were determined from high precision LiDAR or photogrammetric-derived topographic data. These elevation measurements therefore have a precision of $\leq$ 1 m, which is well within the natural variability in the height of shorelines formed above a still water plane (Atwood, 1994; Adams and Wesnousky, 1998).

To augment the geologic records of lake-level fluctuations, we applied paleohydrologic models to gain additional insight into timing, rates, and magnitudes of hydrologic changes. For Walker Lake, annual streamflow was simulated using the tree-ring chronologies contained within the LBDA that, in turn, was routed to a Walker Lake water balance model that also runs in annual time steps, similar to the approach used by Adams et al. (2015) for Tulare Lake in California. In this case, the combined annual flow volume recorded at two stream gauges along the East Walker River (10293000) and West Walker River (10296500) were regressed against LBDA-derived PDSI values from a grid point (GP 2239; Fig. 1) located in the headwaters of the Walker River to develop statistical relationships between annual tree growth and stream flow. These relationships enabled estimates of annual flow volumes of the Walker River over the last 2000 years. This approach is justified because most of the water utilized by the trees during the growth season comes from snowmelt, which also controls annual river discharge. The simulated annual river flows were in turn routed to a Walker Lake water balance model,

constrained by the hypsometry of the basin (Lopes and Smith, 2007), to simulate lake-level fluctuations over this same period.

The water balance model was calibrated by using annual gauged flow recorded at the lowest gauge (10302002) along the Walker River, which is below all points of diversion or storage, along with PRISM estimates of precipitation (Daly et al., 2008) on the lake as input, and a randomly varied lake-evaporation rate between 125 - 135 cm/yr (Milne, 1987) controlling the output. To assess the reasonableness of the water balance model, simulated lake-level changes were compared to actual lake-level changes over the 1995 – 2017 period of record for the gauge. Historical lake-level changes could not be simulated prior to 1995 because the total volume of water actually reaching the lake was not accurately recorded.

This same coupled modeling approach was attempted for the Carson Sink but the volumes of modeled flow were insufficient to account for the large lakes present at various times in the late Holocene. Instead, the relatively simple lake water balance models of Adams (2003) were updated to address the questions of what volumes of stream discharge were necessary over what periods of time to produce the late Holocene lakes.

RESULTS

Walker Lake

The geologic mapping of House and Adams (2009, 2010) demonstrated that the undated but late Holocene highstand at Walker Lake was at about 1262 m, based on beach ridges developed on post-Lahontan highstand alluvial fans (Fig. 3). Further, these beach ridges

273 are at about the same elevation as a sill with a channel leading to the Double Springs
274 subbasin to the northeast of Walker Lake (Fig. 2). Although this subbasin is relatively
275 small (36 km^2 and 0.48 km^3 when full), it apparently accommodated all overflow when
276 Walker Lake was at the 1261 m sill, thereby restricting late Holocene levels to this
277 elevation and below.

278 To augment the Walker Lake-level record of Adams (2007), luminescence samples
279 were collected from a suite of beach ridges located in the northwestern part of the basin
280 that range in elevation from about 1252 to 1262 m (Figs. 2 and 3). The beach ridges are
281 primarily composed of granitic sand and grit with small angular to subangular gravel
282 clasts ($\leq$ 5 cm) likely reworked from existing alluvial fan deposits and older beach
283 deposits. The surfaces of the upper beach ridges (1262 m, 1261 m, and 1260 m; Fig. 3) in
284 this sequence are partially covered by a loose, poorly developed pavement or patches of
285 discontinuous cryptogamic crust preferentially developed around the bases of widely
286 spaced (1-5 m) desert shrubs. Soil development is minimal, consisting of small amounts
287 of eolian silt and fine sand infiltrating into the upper parts ($\leq$ 20 cm) of the beach ridges,
288 but not enough has accumulated to develop Av horizons. Sample pits dug either on the
289 barrier crests or slightly lakeward revealed an internal structure consisting of laminae to
290 thin beds ($\leq$ 5 cm) of sand and fine gravel gently dipping to the south toward the former
291 lake, with local heavy mineral concentrations along the laminae. The lower beach ridges
292 (1257 m, 1253 m, and 1252 m; Fig. 3) lack the loose pavements, patchy cryptogamic
293 crusts, and infiltrated dust that characterize the upper beach ridges, but their internal
294 structure is similar. The surface and soil characteristics of all of these beach ridges are
295 consistent with a late Holocene age, when compared to the typical characteristics

displayed by Lahontan highstand beach features (~15,500 cal yr BP) in the area that possess better developed pavements and stronger soil development (Adams and Wesnousky, 1999)

Results from the luminescence samples are also consistent with a late Holocene age, with the upper most and oldest beach ridge (1262 m) dating from about 3620 $\pm$ 300 cal yr BP (Table 3 and Fig. 3), based on two samples. Although the duplicate sample ages from each of the lower beach ridges show wider scatter, each group overlaps within 1-sigma uncertainty, except for those from the 1257 m ridge for which 90 years separates the 1-sigma age ranges (Table 3).

Based on the luminescence ages and their uncertainties, the 1262, 1261, and 1260 m beach ridges were most likely formed between about 3300 – 4000 cal yr BP, and the 1257 m ridge formed between 2000 and 3000 cal yr BP. The 1253 m ridge formed about 1000 cal yr BP (Table 3 and Fig. 3). All of these beach ridges are above the historical highstand of 1252 m (Adams, 2007). The new ages and elevations of the beach ridges were combined with lake-level data from Adams (2007) to revise the Walker Lake-level curve for the last 4500 years (Fig. 4). Most of the changes were made in the older part of the curve, accounting for the ages and elevations of the beach ridges dated in this study. Particularly uncertain parts of the curve are labeled with question marks.

Carson Sink

As part of their efforts to map the surficial geology of the Lahontan Mountains and to apply modern dating methods to the Quaternary stratigraphy originally defined by Morrison (1964, 1991), Bell and House (2010) and Bell et al. (2010) documented several

319 stratigraphic sections and deposits that reflect late Holocene lake-level changes in the
320 Carson Sink. The two main sites include one above the northeast shore of Carson Lake at
321 Macari Lane and the other along Grimes Point Slough, which connects Carson Lake with
322 the rest of the Carson Sink via the Stillwater Marsh (Fig. 2). Four additional radiocarbon
323 samples bearing on late Holocene lake levels were collected by Bell et al. (2010) from
324 other sites in the area (Table 2).

325 The Macari Lane and Grimes Point Slough sections are similar and consist of thin to
326 medium beds of brown silty sands with aquatic mollusks interbedded with thin beds of
327 dark gray organic-rich silts that Bell et al. (2010) interpreted as interbedded lacustrine,
328 marsh, and fluvial sediments. We used the elevations and ages of these units combined
329 with the ages of the 1202 m and 1198 m beaches in the area (Adams, 2003) to reconstruct
330 lake-level fluctuations in the Carson Sink over the last 5000 years.

331 Figure 5 presents the late Holocene Carson Sink lake-level curve that is based on a
332 synthesis of all relevant radiocarbon ages (Table 2). In this curve, radiocarbon samples
333 from lacustrine sediments within the Carson Lake subbasin but above the outlet elevation
334 (~1195 m) indicate lakes that probably encompassed much of the Carson Sink. These
335 lakes attained highstands during the intervals 660 – 910, 1310 – 1520, 1570 – 1820, 1730
336 – 1940, and 2350 – 2700 cal yr BP (Table 2 and Fig. 5). The lacustrine samples dating
337 from about 550 - 760, 2000 - 2300, and 3730 - 4080 cal yr BP were collected from sites
338 within the main body of the Carson Sink.

339 We refined the timing of five of the highstands by using tree ring records as an
340 indicator of wet periods (Cook et al., 2010). The end year of each of the five youngest
341 wet periods is 663, 829, 1439, 1593, and 1909 cal yr BP, respectively. Judging from the

342 tree ring records, these periods of elevated lake levels lasted from about 20 to 50 years
343 (Fig. 5).
344
345 **Walker River paleochannel**
346 There are multiple channel traces in Mason Valley marking past courses of the Walker
347 River. The Walker River paleochannel is defined as the one that can be almost
348 continuously traced from where it splits from the modern Walker River in southern
349 Mason Valley and then flows northwest through Adrian Valley to connect with the
350 Carson River (Fig. 2). This channel has probably accommodated the most recent flows
351 during diversions. Although the area of the channel bifurcation is now a smooth
352 agricultural field, the natural elevation difference between the paleochannel and the
353 modern Walker River is only one to two meters. Two sites along the paleochannel give
354 evidence for water flowing toward the Carson Sink, but do not necessarily exclude the
355 possibility that water was also flowing into Walker Lake at the same time.
356
357 *Perazzo Slough site*
358 The Perazzo Slough site is located in northwest Mason Valley along the paleochannel
359 where a drainage ditch cuts across a series of meanders (Figs. 6A and 6B), exposing a
360 cross section through the fluvial landforms and stratigraphy. The sediments primarily
361 consist of thin to medium cross-bedded fine to coarse sands with thin discontinuous
362 lenses of silt or fine gravel. These sequences form discrete packages separated by angular
363 buttress unconformities (Fig. 6A). Some packages have thin mud layers at their bases that
364 contain abundant organic material including charcoal. The arrangement of the

365 sedimentary units (numbered i – vi, in order of increasing relative age) conforms to the
366 surface morphology where the youngest channel unit (i) spans the width of the surface
367 channel and is inset into older units (ii and iv) whose edges conform to the bases of
368 terrace risers on the surface (Figs. 6A and 6B). The different stratigraphic units are
369 interpreted as a series of inset channel and point bar deposits that reflect different periods
370 when the Walker River was flowing through the paleochannel. According to the
371 radiocarbon ages of these units, this channel was active several times between about 1520
372 and 930 cal yr BP (Fig. 6A; Table 2).
373
374 *Adrian Valley-Carson River confluence*
375 At the north end of Adrian Valley, the Walker River paleochannel becomes a tributary to
376 the Carson River at the Adrian Valley-Carson River confluence (Figs. 2, 6C, and 6D). A
377 five-meter-high cutbank into this terrace on the south side of the Carson River exposes a
378 cross section through the stratigraphy of the paleochannel (Fig. 6C).
379 The predominately fine to coarse sandy sediments exposed here are arranged into
380 discrete packages separated by angular buttress unconformities. The units are numbered
381 from 1 to 10 in order of increasing age (Fig. 6C). Unit 10 is the oldest in the exposure and
382 consists of horizontal thin to medium bedded sands, silty sands, and organic and
383 charcoal-rich silty muds. This unit is interpreted to represent vertical accretion of Carson
384 River floodplain deposits from about 970 to 680 cal yr BP (Fig. 6C). On the east side of
385 the exposure, a series of inset channel units are exposed in cross section and generally
386 young to the east. The two radiocarbon ages from these units indicate that they were
387 deposited within the last 430 cal yr BP, which is consistent with the age of unit 10. The

388 sandy sediments are arranged into thin to medium beds that generally parallel the base of
389 each unit (Fig. 6C) and show common cross-bedding and current ripple cross-
390 laminations. Whereas the oldest of these inset channel deposits are graded to a level at
391 about the modern Carson River channel, the younger channels appear to be graded to
392 progressively higher base levels. The age of channel unit 9 is younger than unit 10, but
393 cannot be directly related to the ages of channel units 1 – 8.
394 Based on their approximately perpendicular orientation to the modern Carson River,
395 and their location at the mouth of Adrian Valley, the inset channels exposed on the east
396 side of the exposure are interpreted to represent paleochannels of the Walker River (Fig.
397 6C). Further, the ages of these sediments indicate that these channels have been active
398 multiple times during the last 1000 years.
399 The presence of Carson River meander scars on the surface of the terrace at the
400 mouth of Adrian Valley (Fig. 6D) suggests the possibility that the inset channels exposed
401 in the cutbank (Fig. 6C) were formed by the Carson River instead of the Walker River.
402 Similar meander scars are characteristic of this terrace surface both upstream and
403 downstream from the confluence, but the only place that inset channels were found in the
404 stratigraphy was at the mouth of Adrian Valley. All of the other terrace exposures
405 examined along the Carson River displayed vertically accreted sediments without
406 evidence of cutting and filling. Although not definitive, the inset channels at the mouth of
407 Adrian Valley are most likely associated with the Walker River paleochannel.
408
409 **Paleohydrological modeling**

410 Paleohydrologic modeling gives estimates of the total annual discharge of the Walker
411 River and the response of Walker Lake to a variety of flow scenarios. The statistical
412 relationship between the PDSI time series from grid point 2239 to the total annual gauged
413 flow in the East Walker and West Walker rivers has an $r^2 = 0.56$ and a standard error of
414 0.13 (Fig. 7a). This relationship was used to reconstruct Walker River discharge for the
415 period 1926 to 2005 that could be directly compared to the gauged flow (Fig. 7b).
416 Although the reconstructed flows match the gauged flows at moderate volumes
417 reasonably well, the reconstructed flows slightly underestimate the largest annual flow
418 volumes and slightly overestimate the lowest gauged flows. Underestimating flow
419 volumes in particularly wet years is a common phenomenon in many streamflow
420 reconstructions (e.g., Meko et al., 2001; Graumlich et al., 2003; Watson et al., 2009;
421 Wise, 2011) because high volume and rapid discharge may not have a lasting effect on
422 soil moisture (Meko and Woodhouse, 2011). Annual precipitation at Walker Lake was
423 simulated for the historical period based on the statistical relationship between PRISM
424 precipitation estimates and the PDSI time series from grid point 2339, which has an $r^2 =$
425 0.48 and a standard error of 28 (Fig. 7c). This relationship was then used to reconstruct
426 annual precipitation at Walker Lake for the period 0 to 2005 AD.
427 To test the Walker Lake water balance model, lake-level fluctuations were modeled
428 for the historical period using gauged flow as well as tree-ring-reconstructed flow as
429 input, along with PRISM precipitation estimates at Walker Lake and an annual
430 evaporation rate ranging between 125 and 135 cm/yr. Although the Siphon gauge
431 (10302002) record is relatively short (1995 – 2017), use of this data in the model results
432 in lake-level fluctuations that closely match actual fluctuations (Fig. 8), supporting the

credibility of the lake water balance model. Lake-level fluctuations that would have occurred during the historical period if water had not been diverted were also modeled by using the combined flows from stream gauges located upstream from major points of diversion (Fig. 8). These hypothetical lake levels, using actual gauge records, are closely matched by modeled lake-level changes derived from tree-ring-reconstructed flow from those same stream gauges. The magnitude of difference between these latter two curves ranges up to one to three meters (Fig. 8), likely indicating the uncertainty in the paleohydrologic modeling procedure (Adams et al., 2015).

Tree ring simulated mean annual Walker River flow volumes and precipitation values at Walker Lake, along with an annual evaporation rate of 125 – 135 cm/yr, were then used to simulate lake-level changes at Walker Lake for the last 2000 years (Fig. 9). Our estimates indicate that lake level quickly rose from a starting elevation of 1225 m at 2000 cal yr BP to fluctuate between 1250 and 1255 m until about 1080 cal yr BP (870 AD) when lake level fell to about 1246 – 1247 m. Lake level remained relatively low until about 950 cal yr BP (1000 AD) when lake level rose in a step-like manner to reach 1255 m by 830 cal yr BP (1120 AD). Lake level dropped to 1248.5 m by about 710 cal yr BP (1240 AD) before rising to fluctuate around 1255 m into the historical period (Fig. 9).

DISCUSSION

The paleohydrologic histories of the Carson Sink and Walker Lake reflect interactions among climate and river dynamics. In particular, these two lake systems are linked by the occasional diversions of the Walker River from Walker Lake to the Carson Sink. Fundamental differences between the Carson Sink and Walker Lake in terms of drainage

456 basin size and location and lake-basin hypsometry have also affected how these basins
457 have responded to climate fluctuations during the Holocene.
458 The Walker River was diverted back into Walker Lake by about 5500 cal yr BP, after
459 spending most of the early and middle Holocene emptying into the Carson Sink (Benson
460 and Thompson, 1987a; Bradbury et al., 1989; Benson et al., 1991). By about 4000 cal yr
461 BP, Walker Lake had reached its highest levels of the Holocene at around 1262 m (Fig.
462 4), coincident with the Neopluvial period that was originally defined by Allison (1982) to
463 indicate a period of relatively high lake levels that coincided with the Neoglacial period
464 (e.g., Denton and Stuiver, 1966; Porter and Denton, 1967). Except for two minor lake
465 level drops to about 1240 – 1245 m, Walker Lake remained at relatively high levels ($\geq$
466 1255 m) until about 2800 cal yr BP (Fig. 4). Benson et al. (1991) indicated that Walker
467 Lake nearly desiccated by around 2000 cal yr BP based on the abundance of ruppia
468 pollen found in a core interval dating from this period, which was interpreted to represent
469 a shallow playa lake. Berelson et al. (2009) suggested that lake level did not fall below
470 about 1200 m at this time, based on the ages and carbonate-associated sulfate content of a
471 low elevation tufa. The timing of this low lake level agrees with evidence for the Late
472 Holocene Dry Period in the Great Basin that extended from about 2900 to 1850 cal yr BP
473 (Mensing et al., 2013), although such low Walker levels may have resulted from
474 diversion of the Walker River into the Carson Sink.
475 From about 1500 cal yr BP to the historical period, Walker Lake has undergone
476 several high amplitude fluctuations, constrained by the age of shorelines or nearshore
477 deposits at relatively high elevations and fluvial deposits or other evidence of desiccation
478 at relatively low elevations (Fig. 4) (Adams, 2007). The elevation of the highstand at

about 1000 cal yr BP (Fig. 4) was adjusted upward from the 2007 curve based on the age of the 1253 m shoreline (Fig. 3 and Table 2).

These late Holocene Walker Lake fluctuations correspond to surface area changes ranging from about 300 to 150 km^2 and volumetric changes ranging from about 13 to 3 km^3. The magnitude of these changes can be placed in perspective by noting the historical decline of Walker Lake from 1252 m in 1868 to 1190 m in 2016, owing to annual reductions in Walker River flow ranging from about 50% to over 90% due to upstream diversions and consumption. The question remains: are late Holocene lake-level fluctuations representative of climate fluctuations or were they caused by changes in the path of the Walker River?

Evidence against strictly climatic factors and for multiple river diversions explaining the dramatic lake-level changes includes discrete packages of different-aged fluvial sediments preserved at two different sites along the Walker River paleochannel (Fig. 6). Each of these packages indicate periods when Walker River water was flowing through the paleochannel into Carson Sink, presumably instead of flowing into Walker Lake, although it is possible that flow was occasionally split between the two channels. The lengths of time or volumes of water that flowed through the paleochannel cannot be determined based on the geologic evidence.

Paleohydrologic modeling bolsters the case for Walker River diversions over the last 2000 years. According to results of the tree-ring based water balance modeling, Walker Lake levels would have remained relatively high (1245 – 1258 m) during the last 2000 years, with only relatively minor fluctuations, particularly through the Medieval Climate Anomaly (Figs. 9 and 10). The physical evidence for much greater Walker Lake-level

fluctuations therefore suggests that river diversions in and out of the Walker basin are likely responsible for the large lake-stage fluctuations. Consequently, the severe climatic conditions that Hatchett et al. (2015) inferred from the large-scale lake-level fluctuations during the Medieval Climate Anomaly may be overstated.

For the Carson Sink, our paleohydrologic models could not simulate geologically-documented high late Holocene lake levels using tree-ring simulated stream flows. Adams (2003) used a simple water balance model (e.g., Benson and Paillet, 1989) in annual time steps to determine that the combined flow of the Humboldt, Carson, and Walker rivers would have only produced lakes below an elevation of about 1188 m (~1660 km^2, 8.4 km^3) during the historical period. To produce a lake approaching 1200 m (~2815 km^2, 35.7 km^3) in the Carson Sink, mean annual flow would have to have increased by a factor of 4 to 5 (3 – 4 km^3/yr) and remained in that range for decades (Adams, 2003). The main constraining factor that limits high lake levels in the Carson Sink is the broad, relatively flat hypsometry of the basin, which causes large increases in lake surface area and evaporative output with relatively minor increases in lake level.

In contrast, the relatively deep and narrow hypsometry of the Walker Lake basin (Lopes and Smith, 2007) indicates that a 50 m increase in lake level from 1200 m to 1250 m results in an increase in surface area from 132 to 304 km^2 and an increase in volume from about 2.3 to 12.8 km^3. The evaporative output from Walker Lake when it is at 1250 m is about 0.4 km^3/yr, which is similar to the mean annual historical flow into the basin (Table 1). The near balance between Walker River inflow and the evaporative output of Walker Lake when it is near 1250 m may explain why Walker Lake would have fluctuated around 1245 - 1255 m during the historical period if upstream water

525 withdrawals had not occurred (Fig. 8) and over the last 2000 years if river diversions had
526 not occurred (Figs. 9 and 10).
527 The tree ring chronologies contained within the LBDA may indicate the timing and
528 duration of high-flow periods sufficient to produce high lake levels in the Carson Sink.
529 Cook et al. (2010) examined precipitation conditions during the Medieval Climate
530 Anomaly and determined that two lengthy droughts in the Great Basin bookended a
531 particularly wet period that lasted 46 years from 1075 to 1121 AD (875 – 829 cal yr BP).
532 Spatially, the wettest part of the Great Basin during the Medieval pluvial was in the
533 headwaters of the Humboldt River where PDSI values averaged 1 to 2 (Cook et al.,
534 2010), while PDSI values in the headwater reaches of the Carson and Walker river basins
535 ranged from 0 – 1 during this period. This particularly wet episode overlaps with the
536 radiocarbon age of the Salt Wells beach barrier (660 – 910 cal yr BP) (Adams, 2003),
537 suggesting that this lake expanded to a surface elevation of about 1200 m during this
538 period. The 46-year duration of the Medieval pluvial constrains the sustained magnitude
539 of flow into the Carson Sink to have been greater than the historical average by about a
540 factor of 4 to 5, based on the modeling of Adams (2003), or similar to the peak annual
541 discharges recorded for the Humboldt and Carson rivers (Table 1). The timing and
542 duration of four other lake stands over the last 2000 years were similarly refined and
543 indicate that discrete pluvial periods affecting the Carson Sink have lasted from 21 to 27
544 years (Fig. 5) and reflect periods of flow that were also much above the historical
545 average. The temporal refinement of the duration of the wet periods in the Carson Sink
546 led to the drawing of sharply peaked lake-level fluctuations on that curve separated by
547 periods of dryness (Fig. 5). Three high lake periods occurred during the Late Holocene

548 Dry Period (2900 to 1850 cal yr BP; Mensing et al., 2013), suggesting that there may
549 have been a few relatively wet periods in this overall dry episode.
550 Based on the historical gauge records, it is apparent that during wet periods the
551 Humboldt River can deliver a higher proportion of water to the Carson Sink, relative to
552 its annual average, than the Carson River does. During the wettest years on record, the
553 Humboldt River delivered 4.4 times its mean average annual flow, whereas the Carson
554 River delivered 2.8 times its mean annual flow during the wettest year on record, even
555 though the mean annual discharges for these rivers are similar (Table 1). This
556 discrepancy may be due to the much larger size of the Humboldt River basin versus the
557 Carson River basin (Fig. 1). Sustained high discharge volumes in both basins may be
558 influenced by increases in the runoff coefficient during extended wet periods (e.g.,
559 Risbey and Entekhabi, 1996; Menking et al., 2004).
560 Figure 10 shows summary plots of lake-level changes in Walker Lake and the Carson
561 Sink, the time periods when water was flowing through the Walker River paleochannel,
562 the timing of drought terminations in the Walker River (Stine, 1994), and
563 paleohydrologic modeling results for Walker Lake. These comparisons indicate that flow
564 through the paleochannel is indeed associated with falling or low Walker Lake levels and
565 sometimes high Carson Sink levels, suggesting that river diversion was at least partly
566 responsible for lake-level fluctuations in both basins. A striking example of this
567 association is during the Medieval pluvial (875 – 829 cal yr BP; Cook et al., 2010), when
568 Walker lake levels were low even though modeling results indicate that Walker should
569 have been rising from about 1245 m to 1250 m at that time. The death age of trees in the
570 Walker River channel near its headwaters indicate the end of the first of the Medieval

droughts at around 830 cal yr BP (Stine, 1994) and the beginning of the Medieval pluvial. The Walker River paleochannel was active during the Medieval pluvial and one of the largest lakes in the late Holocene appeared in the Carson Sink, all of which suggests that the Walker River was augmenting the flows of the Carson and Humboldt at this time. Relatively high lake levels during the Medieval pluvial were also recorded at Mono Lake (Stine, 1990) and Owens Lake (Bacon et al., 2018).

CONCLUSIONS

This study synthesizes existing data on the late Holocene lake-level histories of the Carson Sink and Walker Lake, augmented by additional dating at key shoreline localities and at sites along the Walker River paleochannel that connects these basins. Moisture-sensitive tree-ring chronologies from the Living Blended Drought Atlas (Cook et al., 2010) were used to refine the timing and duration of high lake levels in the Carson Sink and to model annual lake-level fluctuations in Walker Lake over the last 2000 years.

Although these basins are in the same general region and are connected by the paleochannel, the details of each of their histories differ in significant ways based on a number of factors. Transient factors include the multiple diversions of the Walker River back and forth between Walker Lake and the Carson Sink, as well as climate variability across these drainage basins that span from the Sierra Nevada to northeast Nevada (Fig. 1).

There are also fundamental differences in some of the physical factors that influence the basin histories, particularly the different hypsometries and drainage basin sizes. The normally dry Carson Sink is broad and flat so that relatively small increases in lake-

surface elevation lead to relatively large increases in surface area and evaporative output, thus acting as a strong negative feedback to higher lake levels. In contrast, the relatively narrow and deep Walker Lake basin would have maintained an average lake-surface elevation of 1245-1255 m over the last 100 years under natural conditions, which corresponds to a surface area just large enough to evaporate enough water to balance the mean annual inflow.

Multiple large-scale (50 $\pm$ m) lake-level fluctuations at Walker Lake in the last 2000 years likely resulted from river diversions. Evidence for this includes the ages of fluvial sediments preserved along the paleochannel that coincide with low Walker Lake levels and tree ring-based paleohydrologic modeling that suggests that lake levels would have been relatively high over the last 2000 years, absent the diversions.

The large lakes that did occasionally appear in the Carson Sink during the late Holocene were created by relatively wet periods that lasted from two to several decades. The largest of these rose during the 46-year long Medieval pluvial centered around 1100 AD. Paleohydrologic modeling suggests that discharge into the Carson Sink must have increased by a factor of four or five and maintained for those decades. In addition to the diversion of the Walker River into the Carson Sink at that time, increased runoff may have also been facilitated by an increase in the runoff coefficient as well as larger parts of the drainage basin contributing runoff.

Regardless of the absolute temporal precision of the lake-level curves presented herein, they probably capture the absolute magnitudes of hydrologic variability possible in these basins under current climate boundary conditions (e.g., Wanner et al., 2008). Reconstructing lake-level fluctuations in closed basins is one of the few ways of

617 documenting the absolute flux of water across the landscape in prehistoric times.
618 Therefore, defining the timing, magnitude, and durations of both dry and wet climate
619 episodes from past lake levels helps to place possible future extremes into context. In this
620 way, knowledge of the recent past essentially informs future possibilities.
621
622 **ACKNOWLEDGEMENTS**
623 This research was supported by National Science Foundation grants EAR 0087840 and
624 EAR 1252225, as well as by the Desert Research Institute, but all analyses and
625 interpretations were made by the authors. We thank Mike Lawson and Chris McGuire for
626 their help in luminescence sample collection, Wendy Barrera and Tom Capaldi for
627 sample preparation, and Nathan Brown for sample preparation and measurements. We
628 also thank Edward Cook for providing a copy of the Great Basin portion of the Living
629 Blended Drought Atlas. Many discussions both in the office and in the field with John
630 Bell are greatly appreciated and helped focus the work. Thanks John Caskey for
631 providing an unpublished radiocarbon age of anodonta shells from the Walker River
632 paleochannel. Reviews by Noah Abramson, Jim O'Connor, Derek Booth and two
633 anonymous reviewers helped improve the clarity and content of the manuscript.
634
635 **REFERENCES**
636 Adams, K.D., 2003, Age and paleoclimatic significance of late Holocene lakes in the
637 Carson Sink, NV, USA: Quaternary Research, v. 60, p. 294-306.

638 Adams, K.D., 2007, Late Holocene sedimentary environments and lake-level fluctuations
639 at Walker Lake, Nevada, USA: Geological Society of America Bulletin, v. 119, p.
640 126-139.
641 Adams, K.D., and Wesnousky, S.G., 1998, Shoreline processes and the age of the Lake
642 Lahontan highstand in the Jessup embayment, Nevada: Geological Society of
643 America Bulletin, v. 110, p. 1318-1332.
644 Adams, K.D., and Wesnousky, S.G., 1999, The Lake Lahontan highstand: Age, surficial
645 characteristics, soil development, and regional shoreline correlation:
646 Geomorphology, v. 30, p. 357-392.
647 Adams, K.D., Wesnousky, S.G., and Bills, B.G., 1999, Isostatic rebound, active faulting,
648 and potential geomorphic effects in the Lake Lahontan basin, Nevada and
649 California: Geological Society of America Bulletin, v. 111, p. 1739-1756.
650 Adams, K.D., Negrini, R.M., Cook, E.R., and Rajagopal, S., 2015, Annually resolved late
651 Holocene paleohydroology of the southern Sierra Nevada and Tulare Lake,
652 California: Water Resources Research, v. 51, p. 1-17.
653 Allander, K.P., Smith, J.L., and Johnson, M.J., 2009, Evapotranspiration from the lower
654 Walker River basin, west-central Nevada, water years 2005-07: U.S. Geological
655 Survey Scientific Investigations Report 2009-5079, 62 p.
656 Allison, I.S., 1982, Geology of pluvial Lake Chewaucan, Lake County, Oregon:
657 Corvallis, OR, Oregon State University Press, 79 p.
658 Atwood, G., 1994, Geomorphology applied to flooding problems of closed-basin lakes -
659 Specifically Great-Salt-Lake, Utah: Geomorphology, v. 10, p. 197-219.

660 Bacon, S.N., Lancaster, N., Stine, S., Rhodes, E.J., McCarley Holder, 2018, A continuous
661 5000-year lake-level record of Owens Lake, south-central Sierra Nevada,
662 California, USA: Quaternary Research, v. 90, no. 2, p. 276-302.
663 Bell, J.W., Caskey, S.J., and House, P.K., 2010, Geologic map of the Lahontan
664 Mountains quadrangle, Churchill County, Nevada (2nd ed.): Nevada Bureau of
665 Mines and Geology Map 168, 1:24,000 scale, 24 p. text.
666 Bell, J.W., and House, P.K., 2010, Geologic map of the Grimes Point quadrangle,
667 Churchill County, Nevada: Nevada Bureau of Mines and Geology Map 173,
668 1:24,000 scale, 24 p. text.
669 Benson, L.V., 1978, Fluctuations in the level of pluvial Lake Lahontan during the last
670 40,000 years: Quaternary Research, v. 9, p. 300-318.
671 Benson, L.V., 1988, Preliminary paleolimnologic data for the Walker Lake subbasin,
672 California and Nevada, U.S. Geological Survey, Water Resources Investigations
673 Report 87-4258, 50 p.
674 Benson, L., 2004, Western Lakes, *in* Gillespie, A.R., Porter, S.C., and Atwater, B.F., eds.,
675 The Quaternary Period in the United States, Volume 1: Developments in
676 Quaternary Sciences: Amsterdam, Elsevier, p. 185-204.
677 Benson, L.V., and Thompson, R.S., 1987a, The physical record of lakes in the Great
678 Basin, *in* Ruddiman, W.F., and Wright, H.E., Jr., eds., North America and
679 adjacent oceans during the last deglaciation: Boulder, CO, United States,
680 Geological Society of America, p. 241-260.
681 Benson, L.V., and Thompson, R.S., 1987b, Lake-level variation in the Lahontan basin for
682 the last 50,000 years: Quaternary Research, v. 28, p. 69-85.

683 Benson, L., and Paillet, F., 1989, The Use of Total Lake-Surface Area as an Indicator of
684 Climatic Change: Examples from the Lahontan Basin: Quaternary Research, v.
685 32, p. 262-275.
686 Benson, L.V., Meyers, P.A., and Spencer, R.J., 1991, Change in the size of Walker Lake
687 during the past 5000 years: Palaeogeography, Palaeoclimatology, Palaeoecology,
688 v. 81, p. 189-214.
689 Berelson, W., Corsetti, F., Johnson, B., Vo, T., and Der, C., 2009, Carbonate-associated
690 sulfate as a proxy for lake level fluctuations: a proof of concept for Walker Lake,
691 Nevada: Journal of Paleolimnology, v. 42, p. 25-36.
692 Bradbury, J.P., Forester, R.M., and Thompson, R.S., 1989, Late Quaternary
693 paleolimnology of Walker Lake, Nevada: Journal of Paleolimnology, v. 1, p. 249-
694 267.
695 Cook, E.R., Seager, R., Heim, R.R.J., Vose, R.S., Herweijer, C., and Woodhouse, C.,
696 2010, Megadroughts in North America: placing IPCC projections of
697 hydroclimatic change in a long-term palaeoclimate context: Journal of Quaternary
698 Science, v. 25, p. 48-61.
699 Daly, C., Halbleib, M., Smith, J., Gibson, W.P., Doggett, M.K., and Taylor, G.H., 2008,
700 Physiographically sensitive mapping of climatological temperature and
701 precipitation across the conterminous United States: International Journal of
702 Climatology, v. 28, p. 2031-2064.
703 Davis, J.O., 1978, Quaternary tephrochronology of the Lake Lahontan area, Nevada and
704 California, University of Nevada, Nevada Archeological Survey Research Paper
705 7, 137 p.

706 Davis, J.O., 1982, Bits and pieces: the last 35,000 years in the Lahontan basin, *in*
707 Madsen, D.B., and O'Connell, J.F., eds., Man and Environment in the Great
708 Basin, Society of American Archeology Papers No. 2, p. 53-75.
709 Denton, G.H., and Stuiver, M., 1966, Neoglacial chronology, northeastern St. Elias
710 Mountains, Canada: American Journal of Science, v. 264, p. 577-599.
711 Graumlich, L. J., M. F. J. Pisaric, L. A. Waggoner, J. Littell, and J. C. King, 2003, Upper
712 Yellowstone River flow and teleconnections with Pacific basin climate variability
713 during the past three centuries: Climatic Change, v. 59, p. 245–262,
714 doi:10.1023/A:1024474627079.
715 Harding, S.T., 1965, Recent variations in the water supply of the western Great Basin:
716 Berkeley, California, Water Resources Center Archives, University of California,
717 225 p.
718 Hatchett, B.J., Boyle, D.P., Putnam, A.E., and Bassett, S.D., 2015, Placing the 2012-2015
719 California-Nevada drought into a paleoclimatic context: Insights from Walker
720 Lake, California-Nevada, USA: Geophysical Research Letters, v. 42, p. 8632-
721 8640.
722 House, P.K., and Adams, K.D., 2009, Preliminary geologic map of the southern part of
723 the lower Walker River area, Mineral County, NV, Nevada Bureau of Mines and
724 Geology Open File Report 09-13, 1:24,000-scale.
725 House, P.K., and Adams, K.D., 2010, Preliminary geologic map of the northern part of
726 the lower Walker River area, Mineral County, NV, Nevada Bureau of Mines and
727 Geology Open-File Report 10-12, 1:24,000-scale.

King, G.Q., 1993, Late Quaternary history of the lower Walker River and its implications for the Lahontan paleolake system: Physical Geography, v. 14, p. 81-96.

King, G.Q., 1996, Geomorphology of a dry valley: Adrian Pass, Lahontan basin, Nevada: Association of Pacific Coasts Geographers Yearbook, v. 58, p. 89-114.

Lopes, T.J., and Smith, J.L.R., 2007, Bathymetry of Walker Lake, West-Central Nevada, USGS Scientific Investigation Report 2007-5012, 26 p.

Meko, D. M., M. D. Therrell, C. H. Baisan, and M. K. Hughes, 2001, Sacramento River flow reconstructed to AD 869 from tree rings: Journal of the American Water Resources Society, v. 37, p. 1029–1039, doi:10.1111/j.1752-1688.2001.tb05530.x.

Meko, D. M., and C. A. Woodhouse, 2011, Application of streamflow reconstruction to water resources management, in Dendroclimatology Progress and Prospects, vol. 11, Developments in Paleoenvironmental Research, M. K. Hughes, T. W. Swetnam, and H. F. Diaz (eds.): Springer, Heidelberg, Germany, p. 231–261.

Menking, K.M., Anderson, R.Y., Shafike, N.G., Syed, K.H., and Allen, B.D., 2004, Wetter or colder during the Last Glacial Maximum? Revisiting the pluvial lake question in southwestern North America: Quaternary Research, v. 62, p. 280-288.

Mensing, S.A., Sharpe, S.E., Tunno, I., Sada, D.W., Thomas, J.M., Starratt, S., and Smith, J., 2013, The late Holocene Dry Period: multiproxy evidence for an extended drought between 2800 and 1850 cal yr BP across the central Great Basin, USA: Quaternary Science Reviews, v. 78, p. 266-282.

Milne, W., 1987, A comparison of reconstructed lake-level records since the mid-1880s of some Great Basin lakes [M.S. thesis]: Golden, Colorado School of Mines.

751 Morrison, R.B., 1964, Lake Lahontan: Geology of the southern Carson Desert, U.S.
752 Geological Survey Professional Paper 401, 156 p.
753 Morrison, R.B., 1991, Quaternary stratigraphic, hydrologic, and climatic history of the
754 Great Basin, with emphasis on Lake Lahontan, Bonneville, and Tecopa, *in*
755 Morrison, R.B., ed., Quaternary nonglacial geology; conterminous U.S.: Boulder,
756 CO, United States, Geological Society of America, p. 283-320.
757 Newton, M.S., and Grossman, E.L., 1988, Late Quaternary chronology of tufa deposits,
758 Walker Lake, Nevada: Journal of Geology, v. 96, p. 417-433.
759 Porter, S.G., and Denton, G.H., 1967, Chronology of Neoglaciation in the North
760 American Cordillera: American Journal of Science, v. 265, p. 177-210.
761 Reheis, M.C., Adams, K.D., Oviatt, C.G., and Bacon, S.N., 2014, Pluvial lakes in the
762 Great Basin of the western United States: A view from the outcrop: Quaternary
763 Science Reviews, v. 97, p. 33-57.
764 Reimer, P.J., Bard, E., Bayliss, A., Beck, J.W., Blackwell, P.G., Bronk Ramsey, C.,
765 Buck, C.E., Cheng, H., Edwards, R.L., Friedrich, M., Grootes, P.M., Guilderson,
766 T.P., Haflidason, H., Hajdas, I., Hatté, C., Heaton, T.J., Hogg, A.G., Hughen,
767 K.A., Kaiser, K.F., Kromer, B., Manning, S.W., Niu, M., Reimer, R.W., Richards,
768 D.A., Scott, E.M., Southon, J.R., Turney, C.S.M., van der Plicht, J., 2013,
769 IntCal13 and MARINE13 radiocarbon age calibration curves 0-50000 years cal
770 BP: Radiocarbon, v. 55, no.4, p. 1869-1887, doi: 10.2458/azu_js_rc.55.16947.
771 Rhodes, E.J., 2015, Dating sediments using potassium feldspar single grain IRSL: Initial
772 methodological considerations: Quaternary International, v. 362, p. 14-22.

773 Risbey, J.S., and Entekhabi, D., 1996, Observed Sacramento Basin streamflow response
774 to precipitation and temperature changes and its relevance to climate impact
775 studies: Journal of Hydrology, v. 184, p. 209-223.
776 Russell, I.C., 1885, Geological history of Lake Lahontan, a Quaternary lake in
777 northwestern Nevada, U.S. Geological Survey Monograph 11, 288 p.
778 Smith, G.I., and Street-Perrott, F.A., 1983, Pluvial lakes of the Western United States, *in*
779 Porter, S.C., ed., The late Pleistocene.: Minneapolis, MN, United States, Univ.
780 Minn. Press, p. 190-212.
781 Stine, S., 1990, Late Holocene fluctuations of Mono Lake, California: Palaeogeography,
782 Palaeoclimatology, Palaeoecology, v. 78, p. 333-381.
783 Stine, S., 1994, Extreme and persistent drought in California and Patagonia during
784 mediaeval time: Nature, v. 369, p. 546-549.
785 Wanner, H., Beer, J., Butikofer, J., Crowley, T.J., Cubasch, U., Fluckiger, J., Goosse, H.,
786 Gosjean, M., Joos, F., Kaplan, J., Kuttel, M., Muller, S., Prentice, I.C., Solomina,
787 O., Stocker, T.F., Tarasov, P., Wagner, M., and Widmann, M., 2008, Mid- to Late
788 Holocene climate change: an overview: Quaternary Science Reviews, v. 27, p.
789 1791-1828.
790 Watson, T. A., F. A. Barnett, S. T. Gray, and G. A. Tootle, 2009, Reconstructed
791 streamflows for the headwaters of the Wind River, Wyoming, United States:
792 Journal of the American Water Resources Association, v. 45, p. 224–236,
793 doi:10.1111/j.1752-1688.2008.00274.x.
794 Wise, E. K., 2010, Tree ring record of streamflow and drought in the upper Snake River:
795 Water Resources Research, v. 46, W11529, doi:10.1029/ 2010WR009282.

796 Yuan, F., Linsley, B.K., Lund, S.P., and McGeehin, J.P., 2004, A 1200 year record of
797 hydrologic variability in the Sierra Nevada from sediments in Walker Lake,
798 Nevada: Geochemistry, Geophysics, Geosystems, v. 5, p. 1-13.
799 Yuan, F., Linsley, B.K., Howe, S.S., Lund, S.P., and McGeehin, J.P., 2006, Late
800 Holocene lake-level fluctuations in Walker Lake, Nevada USA: Palaeogeography,
801 Palaeoclimatology, Palaeoecology, v. 240, p. 497-507.
802

FIGURE CAPTIONS

Figure 1. Overview map of the Carson Sink and Walker Lake drainage basins (black lines) showing the locations of features and sites mentioned in the text. Background is PRISM mean annual precipitation (Daly et al., 2008) draped over a hillshaded digital elevation model. The green dots represent Living Blended Drought Atlas grid points from Cook et al. (2010), with labels indicating the ones used in this study. The inset map shows the distribution of tree ring chronologies utilized in the LBDA with chronologies extending over the last 500 years shown by black crosses, chronologies covering the years 500–1500 A.D. shown by filled green circles, and chronologies that are older than 500 A.D. shown by filled black triangles. For the full explanation of color symbols, see the online version.

Figure 2. Map of the Carson Sink and Walker Lake basins showing the relevant hydrographic features influencing late Holocene paleohydrology and locations mentioned in text. Medium blue shading in the basins shows the largest extent of late Holocene lakes, while the lighter blue shading indicates the modern extent of water bodies. White outlines show the extent of historical highstands which occurred in 1862 in the Carson Sink and 1868 in Walker Lake. The 1985 lake extent (~1183 m) is also shown in the Carson Sink by a black line. For the full explanation of color symbols, see the online version.

Figure 3. Geomorphic map of a series of late Holocene beach ridges (blue lines) in the northwest Walker Lake basin showing the results of luminescence dating. The historical

826 highstand reached an elevation of 1252 m and shorelines from 1253 to 1262 m date from
827 the late Holocene. Luminescence ages have been converted to years BP (Table 3). For the
828 full explanation of color symbols, see the online version.
829
830 Figure 4. Late Holocene lake-level curve for Walker Lake modified from Adams (2007).
831 Chronological data constraining this curve are found in Tables 2 and 3. The vertical grey
832 band represents the timing of the Medieval Climate Anomaly.
833
834 Figure 5. Late Holocene lake-level curve for the Carson Sink constructed from data in
835 Table 2. The outlet elevation of Carson Lake is at about 1195 m. The blue diamonds
836 represent lakes that flooded the entire Carson Sink, whereas the purple squares represent
837 lakes that may have only filled Carson Lake (see figure 2). Green circles represent fluvial
838 deposits along Grimes Point Slough and the orange triangle represents the historical
839 highstand in 1862. The groups of three red crosses represent the beginning, peak, and end
840 of pluvial periods derived from the LBDA (grid point 2748). Each of these pluvial
841 periods is labeled with the duration in years. The vertical grey band represents the timing
842 of the Medieval Climate Anomaly.
843
844 Figure 6. Cross-sections and maps of the two sites along the Walker River paleochannel
845 (see figure 2). A) Interpreted cross-section of the Perazzo Slough site showing discrete
846 packages of fluvial sediments related to flow along the paleochannel. Relative age
847 increases from i – vi. Width of the exposure is about 80 m. B) Lidar hillshade map
848 showing the Perazzo Slough site, associated fluvial features, and location of the cross-

849 section. C) Cross section exposed along the right bank of the Carson River at the mouth
850 of Adrian Valley (D) showing a series of stacked channel features incised into
851 horizontally bedded flood plain sediments of the Carson River that are interpreted to
852 represent paleochannel deposits of the Walker River. Relative age of stratigraphic units
853 increases from 1 – 10. Exposure is about 5 m high and 90 m long. For the full explanation
854 of color symbols, see the online version.
855
856 Figure 7a. Relationship between LBDA PDSI values (grid point 2239) and annual
857 discharge of the East and West Walker River from 1958-2005. 7b. Reconstructed annual
858 discharge of the Walker River compared to gauged discharge for the period 1926-2005.
859 7c. Plot showing the relationship between PRISM water year annual precipitation and
860 annual PDSI values from grid point 2339 at Walker Lake.
861
862 Figure 8. Modeled Walker Lake-level fluctuations compared to actual lake-level
863 fluctuations for the period 1943-2017 using various simulated and observational data.
864 The solid blue line represents observed lake-level changes, whereas the red dashed line
865 represents modeled changes using discharge from the lowest gauge on the system, which
866 effectively represents the actual volumes of water delivered to the lake. The upper purple
867 dotted line represents lake levels that would have occurred had there been no
868 anthropogenic water withdrawals or consumption on the system by using discharge data
869 from gauges located upstream from points of diversion. The dashed green line represents
870 hypothetical lake-level changes using LBDA-derived discharge from the relationship

871 shown in figure 7a. All model simulations had a starting lake-surface elevation of 1224
872 m. For the full explanation of color symbols, see the online version.
873
874 Figure 9. Plot showing simulated Walker Lake-level changes using PDSI-derived
875 discharge for the period 1950 – 0 cal yr BP. On-lake precipitation was simulated using
876 the relationship in figure 7c.
877
878 Figure 10. Late Holocene lake-level curves for Walker Lake (A) and the Carson Sink (B)
879 along with (i) Walker River paleochannel dates, (ii) Drought terminations in the Walker
880 River basin (Stine, 1994), and (iii) Modeled Walker Lake fluctuations. The vertical grey
881 band represents the timing of the Medieval Climate Anomaly (MCA). The timing of flow
882 episodes in the paleochannel is consistent with Walker Lake lowstands, indicating the
883 Walker River was diverted to the Carson Sink at those times.

Table 1. Stream flow statistics for the Walker, Carson, and Humboldt rivers.

River	Gauge station number	Period of record	Mean discharge (km^3/yr)	Peak discharge (km^3/yr) (Year)
Walker	10293000	1926-2017	0.38	0.96 (2017)
	10296500			
Carson	10309000	1940-2017	0.42	1.17 (2017)
	10310000			
Humboldt	10322500	1946-2017	0.46	2.03 (1984)
	10324500			
	10329000			
	10329500			

Table 2. Radiocarbon ages from the Carson Sink, Walker Lake, and the Walker River paleochannel used in this study.

Setting or location	Sample #	Sample material	Age (^{14}C yr BP)	Age (cal yr BP) (2σ)[a]	Median probability	Elevation (m)	References
Carson Sink							
Humboldt Bar	Beta-68523	Mollusk shell	710	550-760	663	1189	King (1996)
Salt Wells beach barrier	AA-42196	Charcoal	810 ± 72	660-910	744	1204	Adams (2003)
Wildcat scarp	Beta-268974	Mollusk shell	940 + 40	770-930	853	1204	Bell et al. (2010)
Salt Wells beach barrier	L-773V	Anodonta shell	1000 ± 100	710-1170	911	1200	Broecker and Kaufman (1965)
Wildcat scarp	GX-29220	Grass	1510 ± 40	1310-1520	1397	1198	Adams (2003)
Grimes Point Slough	Beta-257495	Snail shell	1550 ± 40	1360-1530	1457	1196.5	Bell et al. (2010)
Wildcat scarp	Beta-259941	Mollusk shell	1770 ± 40	1570-1820	1682	1204	Bell et al. (2010)
Stillwater slough	Beta-257494	Carbonaceous sediment	1830 + 40	1630-1870	1767	1196	Bell et al. (2010)
Macari Lane	Beta-256298	Snail shell	1910 ± 40	1730-1940	1856	1197	Bell et al. (2010)
Macari Lane	Beta-259940	Carbonaceous sediment	2000 ± 40	1870-2060	1951	1196.5	Bell et al. (2010)
Grimes Point Slough	Beta-258558	Snail shell	2130 ± 40	2000-2300	2112	1195	Bell et al. (2010)
Macari Lane	Beta-256297	Mollusk shell	2430 ± 40	2350-2700	2479	1196.5	Bell et al. (2010)
Macari Lane	CAMS-167168	Anodonta shell	2460 ± 40	2360-2710	2553	1196.5	This study
Macari Lane	Beta-256296	Carbonaceous sediment	3510 ± 40	3650-3890	3779	1196	Bell et al. (2010)
N. of Sehoo Mt.	Beta-258556	Snail shell	3600 ± 40	3730-4080	3908	1196	Bell et al. (2010)
Grimes Point Slough	Beta-257493	Carbonaceous sediment	3960 ± 40	4290-4520	4427	1194	Bell et al. (2010)
Walker Lake							
Deltaic foresets	Beta-184830	Charcoal	80 ± 30	30-140	105	1251.5	Adams (2007)
Beach backsets	Beta-184829	Charcoal	250 ± 30	270-320	296	1210	Adams (2007)
Fluvial deposits	AA50385	Charcoal	760 ± 44	650-780	696	1252	Adams (2007)
Wave-rippled sands	Beta-183894	Charcoal	870 ± 40	700-910	781	1224	Adams (2007)
Rooted stump	?	Wood	980 ± 40	800-960	873	1212	Benson and Thompson (1987b)
Fluvial deposits	Beta-184828	Charcoal	1010 ± 40	800-1050	930	1209	Adams (2007)
Wave-rippled sands	Beta-183891	Charcoal	1020 ± 40	800-1050	939	1212	Adams (2007)
Wave-rippled sands	Beta-183890	Plant debris	1040 ± 40	830-1060	954	1211.5	Adams (2007)
Wave-rippled sands	Beta-183893	Charcoal	1040 ± 40	830-1060	954	1223	Adams (2007)
Wave-rippled sands	AA50387	Charcoal	1075 ± 43	920-1070	987	1209	Adams (2007)
Fluvial deposits	Beta-183892	Charcoal	1360 ± 70	1090-1400	1281	1212	Adams (2007)
Fluvial deposits	AA50384	Charcoal	1613 ± 34	1410-1570	1493	1247.5	Adams (2007)
Fluvial deposits	AA50800	Charcoal	2929 + 35	2960-3170	3079	1242	Adams (2007)
Deltaic foresets	AA50386	Charcoal	3242 ± 51	3370-3580	3469	1245.5	Adams (2007)
Walker River paleochannel							
Perazzo Slough	Beta-182940	Charcoal	1100 ± 40	930-1090	1009	NA	This study
Perazzo Slough	Beta-182943	Charcoal	1220 ± 40	1060-1270	1149	NA	This study
Perazzo Slough	Beta-182941	Charcoal	1520 ± 40	1330-1520	1409	NA	This study
Adrian Valley	Beta-66680	Anodonta shell	170 ± 60	0-300	168	NA	King (1996)
Adrian Valley	Beta-66679	Anodonta shell	300 ± 60	0 - 10 150 - 170 280 - 500	378		King (1996)
Adrian Valley	GX-28298	Anodonta shell	330 ± 60	290-500	392	NA	John Caskey, per. comm. (2004)
Adrian-Carson confluence	AA-44042	Wood	195 ± 46	0-310	180	NA	This study
Adrian-Carson confluence	AA-44044	Wood	223 ± 47	0-430	201	NA	This study
Adrian-Carson confluence	AA-53369	Charcoal	820 ± 33	680-790	729	NA	This study
Adrian-Carson confluence	AA-53368	Charcoal	850 ± 33	690-900	757	NA	This study
Adrian-Carson confluence	AA-44043	Wood	965 ± 58	740-970	863	NA	This study

[a]All radiocarbon ages calibrated with Calib 7.1 using the IntCal13 calibration curve (Reimer et al., 2013).

Table 3. Walker Lake luminescence sample locations, ages, and barrier elevations.

Field sample #	Lab #	Easting[a]	Northing[a]	elevation (m)	depth (m)	K (%)	U (ppm)	Th (ppm)	dose rate (Gy/ka)	dose rate		1 sigma uncertainty	Age (years before 2014)	Age, adjusted to 1950 AD (BP)		1 sigma uncertainty
WL13-01	J0563	344373	4309384	1262	0.23	2.7	1.77	7.8	0.27	4.51	±	0.28	3680	3616	±	300
WL13-02	J0564	344373	4309384	1262	0.30	2.7	1.67	7.5	0.26	4.51	±	0.28	3690	3626	±	300
WL13-03	J0565	344494	4309376	1261	0.40	2.5	2.43	8.1	0.25	4.57	±	0.26	4100	4036	±	320
WL13-04	J0566	344494	4309376	1261	0.42	2.6	1.82	7.0	0.25	4.54	±	0.26	3540	3476	±	300
WL13-05	J0567	344429	4309220	1260	0.27	2.3	2.33	7.8	0.26	4.45	±	0.24	3400	3336	±	260
WL13-06	J0568	344429	4309220	1260	0.55	2.5	1.86	6.8	0.25	4.50	±	0.25	3610	3546	±	290
WL13-07	J0569	344429	4309220	1260	0.80	2.1	2.06	7.3	0.24	4.25	±	0.22	3140	3076	±	240
WL13-08	J0570	344540	4309193	1257	0.10	3.0	1.85	5.8	0.31	4.75	±	0.37	2780	2716	±	340
WL13-09	J0571	344542	4309187	1257	0.26	3.0	1.79	5.8	0.28	4.94	±	0.31	2120	2056	±	230
WL13-10	J0572	344532	4308598	1253	0.16	3.4	1.90	8.7	0.28	5.12	±	0.35	1030	966	±	120
WL13-11	J0573	344532	4308598	1253	0.16	3.4	1.97	8.5	0.28	5.13	±	0.35	1230	1166	±	150

[a]UTM coordinates are all in Zone 11 NAD83

Figure 1

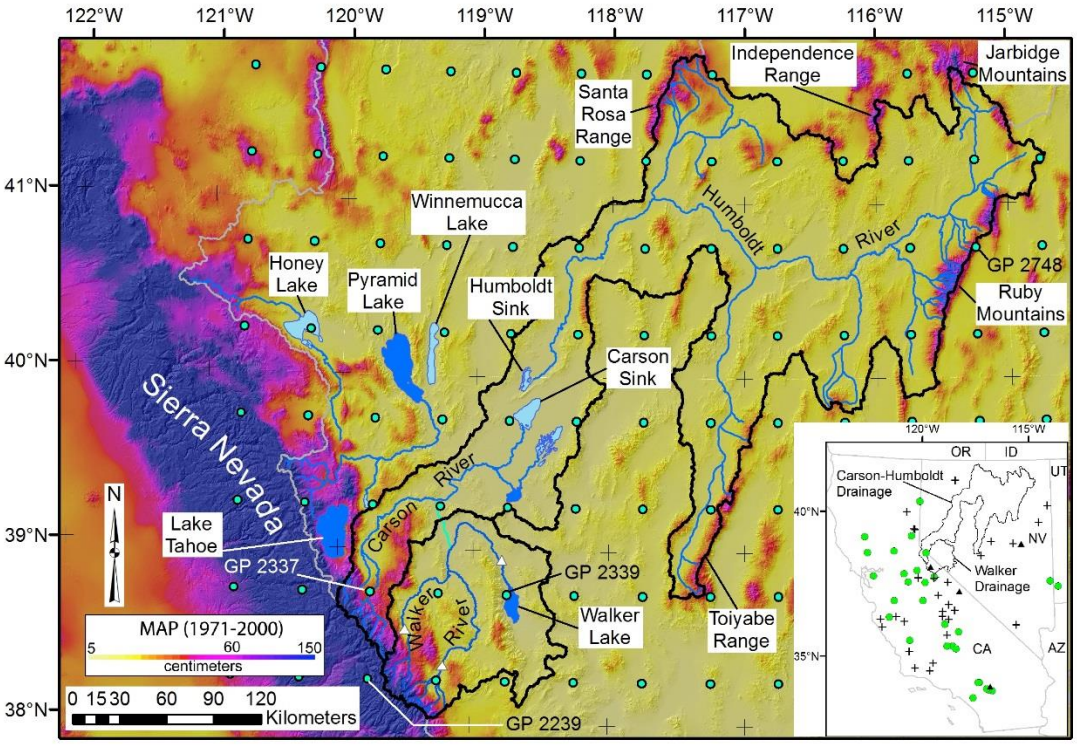
122°W
121°W
120°W
119°W
118°W
117°W
116°W
115°W
41°N
40°N
39°N
38°N
Independence Range
Jarbidge Mountains
Santa Rosa Range
Winnemucca Lake
Honey Lake
Pyramid Lake
Humboldt Sink
Humboldt River
GP 2748
Ruby Mountains
Carson Sink
Sierra Nevada
Carson River
Lake Tahoe
GP 2337
GP 2339
Walker River
Walker Lake
Toiyabe Range
GP 2239
N
MAP (1971-2000)
5
60
150
centimeters
0 15 30 60 90 120
Kilometers
120°W
115°W
40°N
35°N
OR
ID
UT
NV
CA
AZ
Carson-Humboldt Drainage
Walker Drainage

Figure 2

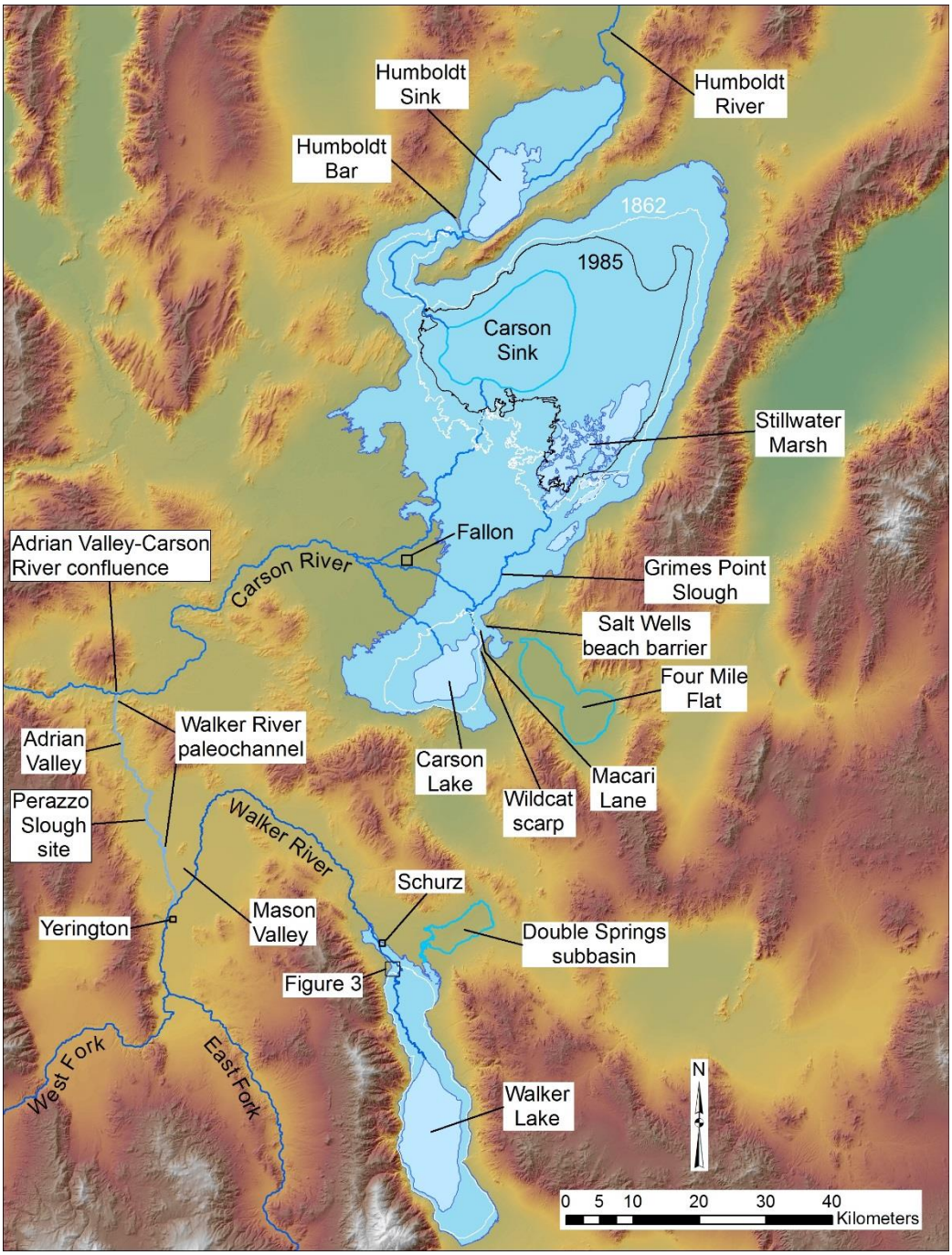
Humboldt Sink
Humboldt River
Humboldt Bar
1862
1985
Carson Sink
Stillwater Marsh
Fallon
Adrian Valley-Carson River confluence
Carson River
Grimes Point Slough
Salt Wells beach barrier
Four Mile Flat
Adrian Valley
Walker River paleochannel
Carson Lake
Macari Lane
Wildcat scarp
Perazzo Slough site
Walker River
Schurz
Yerington
Mason Valley
Double Springs subbasin
Figure 3
West Fork
East Fork
Walker Lake
N
0 5 10 20 30 40
Kilometers

Figure 3

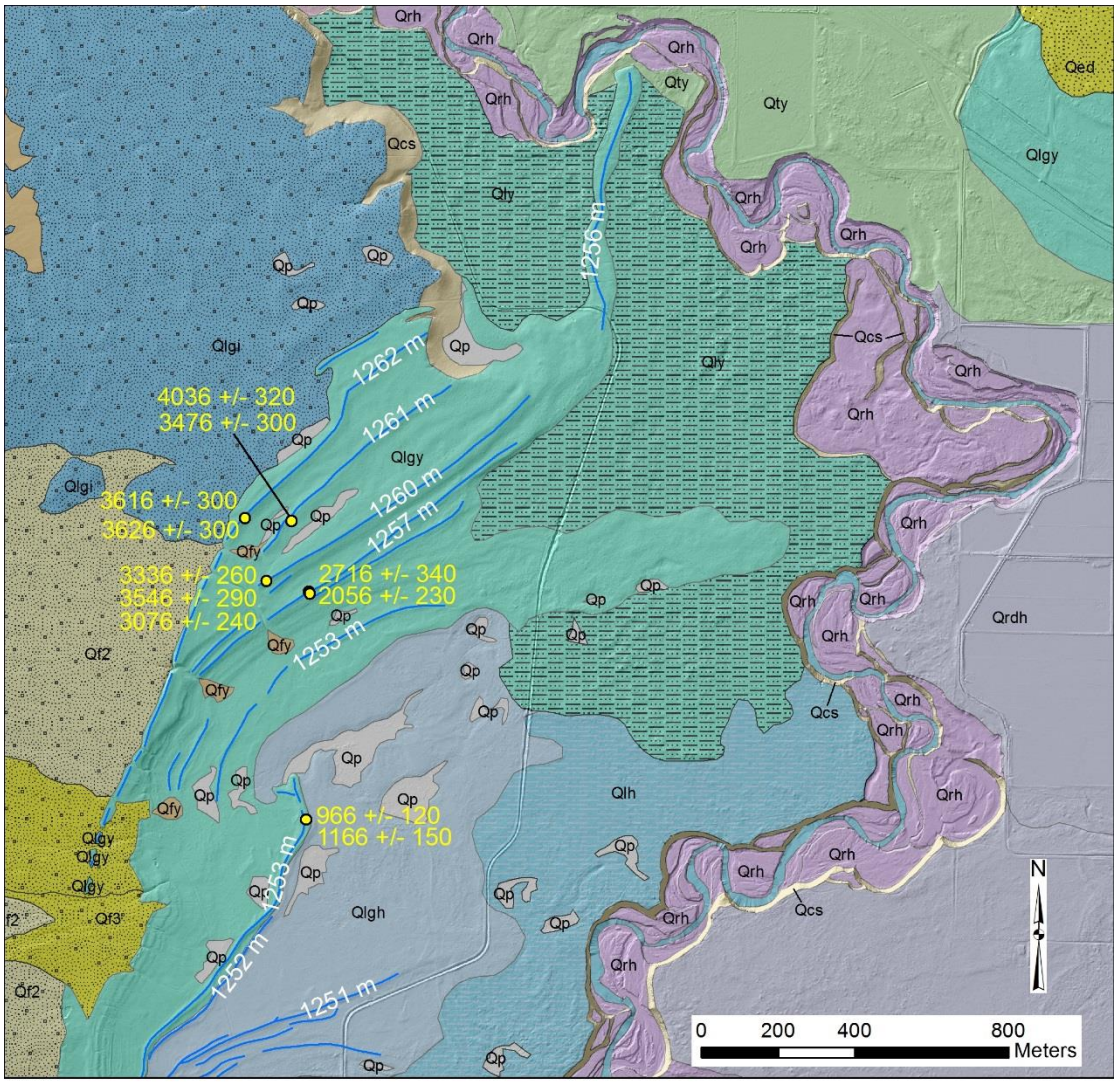

Legend

- Qed Sand dunes
- Qp Playette
- Qcs Scarp colluvium
- Qf3 Alluvial fan (< 3.6 ka)
- Qf2 Alluvial fan (<15.5 ka, > 3.6 ka)
- Qfy Alluvial fan (Holocene)
- Qrh Historical river deposits and terraces
- Qrdh Historical delta deposits
- Qty Fluvial terraces (late Holocene)
- Qlgh Beach gravel (Historical)
- Qlh Fine lacustrine deposits (Historical)
- Qlgy Beach gravel (late Holocene)
- Qly Fine lacustrine deposits (Late Holocene)
- Qlgi Beach gravel (late Pleistocene)

Figure 4

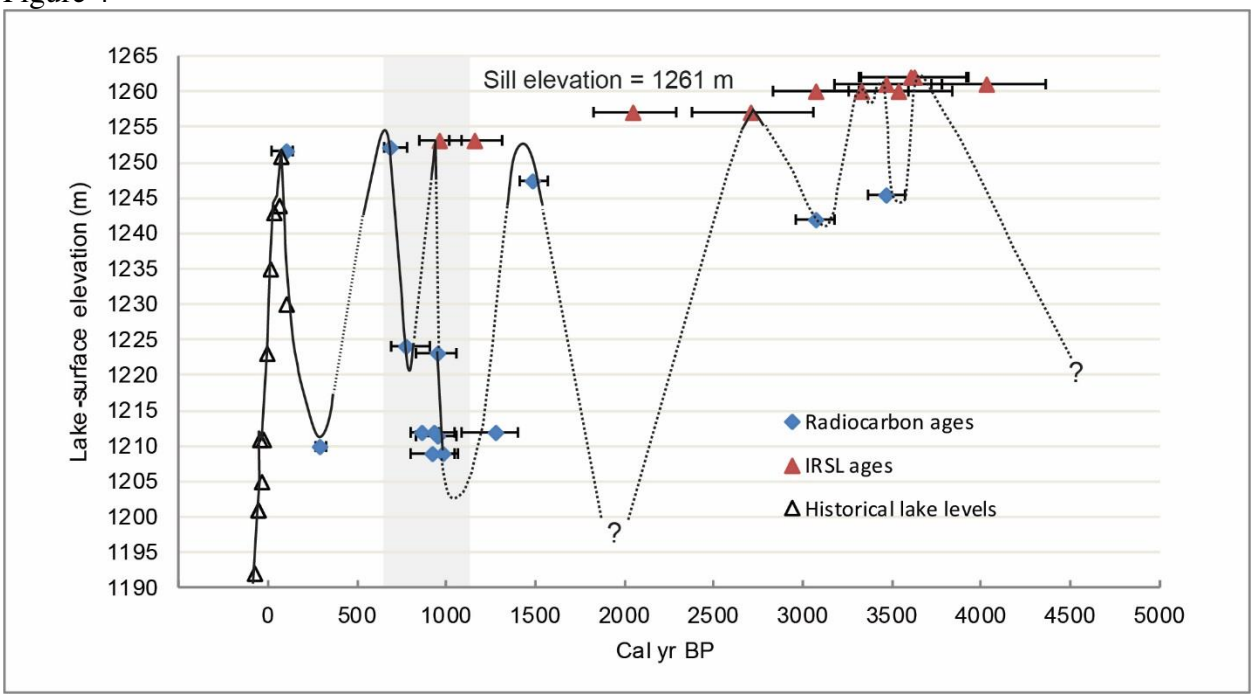
Sill elevation = 1261 m
Lake-surface elevation (m)
1265
1260
1255
1250
1245
1240
1235
1230
1225
1220
1215
1210
1205
1200
1195
1190
0
500
1000
1500
2000
2500
3000
3500
4000
4500
5000
Cal yr BP
Radiocarbon ages
IRSL ages
Historical lake levels
?
?

Figure 5

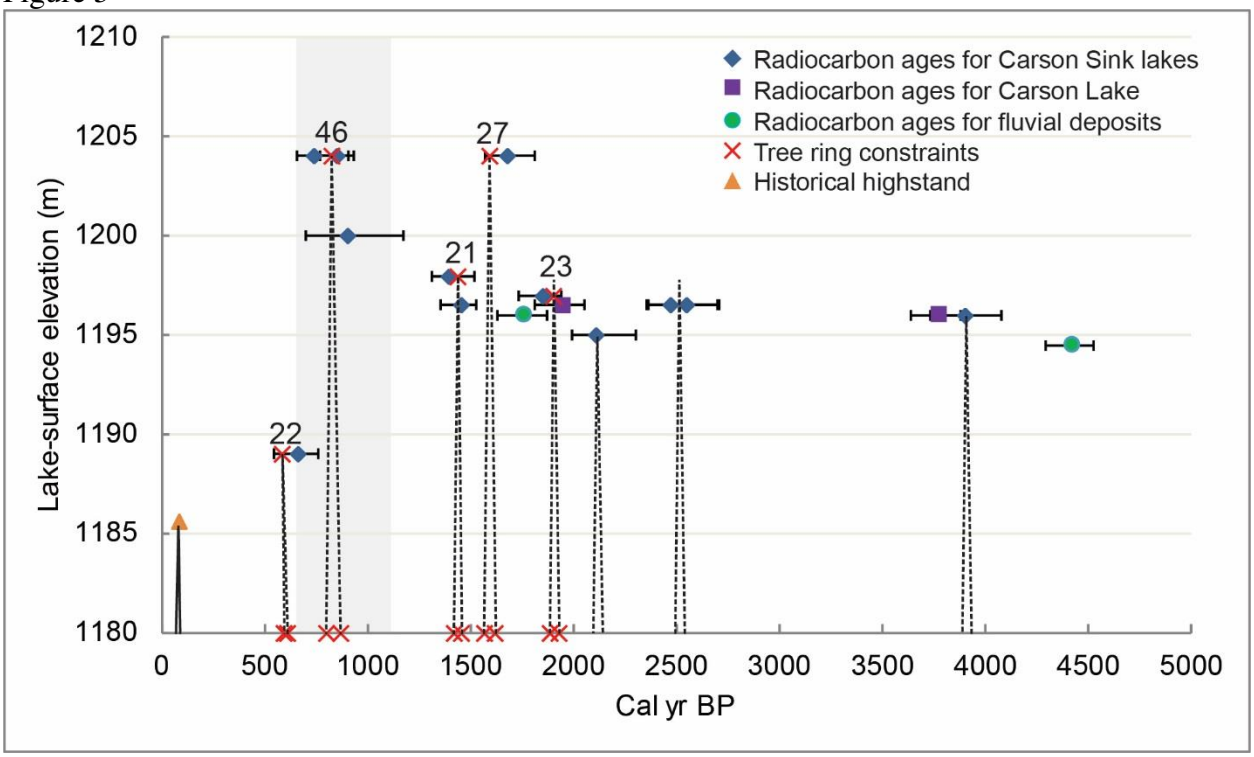
Radiocarbon ages for Carson Sink lakes
Radiocarbon ages for Carson Lake
Radiocarbon ages for fluvial deposits
Tree ring constraints
Historical highstand
46
27
21
23
22
Lake-surface elevation (m)
1210
1205
1200
1195
1190
1185
1180
0
500
1000
1500
2000
2500
3000
3500
4000
4500
5000
Cal yr BP

Figure 6

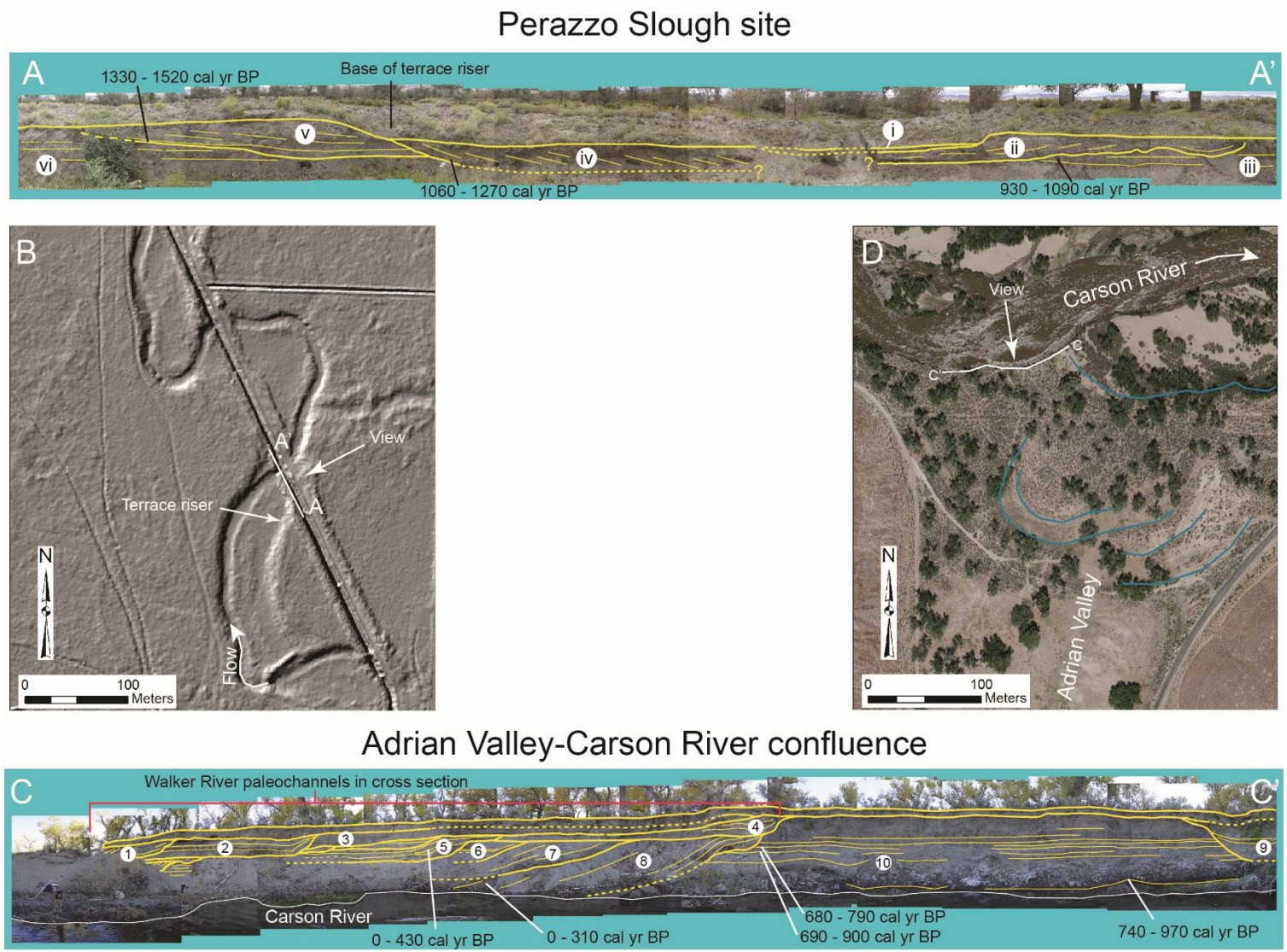
Perazzo Slough site
A
A'
1330 - 1520 cal yr BP
Base of terrace riser
v
vi
iv
i
ii
iii
1060 - 1270 cal yr BP
930 - 1090 cal yr BP
B
A'
View
A
Terrace riser
N
Flow
0
100
Meters
D
View
Carson River
C
C'
N
Adrian Valley
0
100
Meters
Adrian Valley-Carson River confluence
C
C'
Walker River paleochannels in cross section
1
2
3
4
5
6
7
8
9
10
Carson River
0 - 430 cal yr BP
0 - 310 cal yr BP
680 - 790 cal yr BP
690 - 900 cal yr BP
740 - 970 cal yr BP

Figure 7

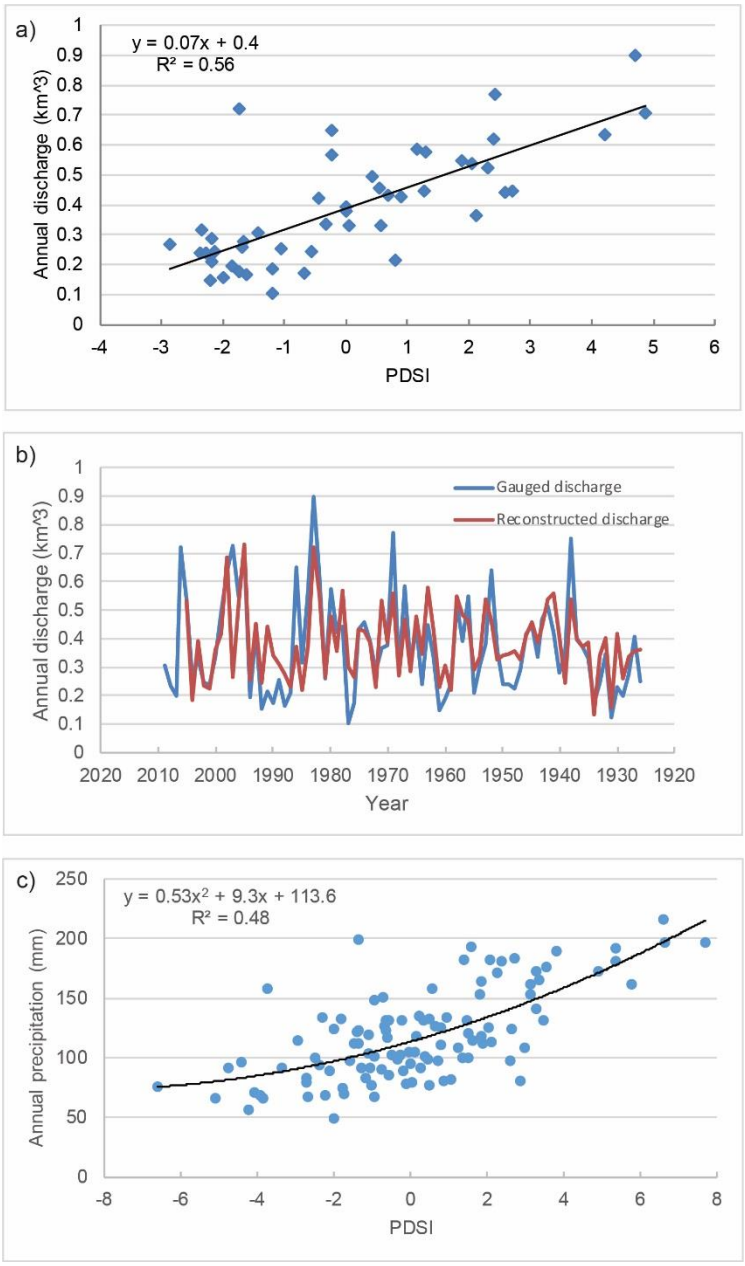
a)
y = 0.07x + 0.4
R² = 0.56
Annual discharge (km^3)
PDSI
b)
Gauged discharge
Reconstructed discharge
Annual discharge (km^3)
Year
c)
y = 0.53x² + 9.3x + 113.6
R² = 0.48
Annual precipitation (mm)
PDSI

Figure 8

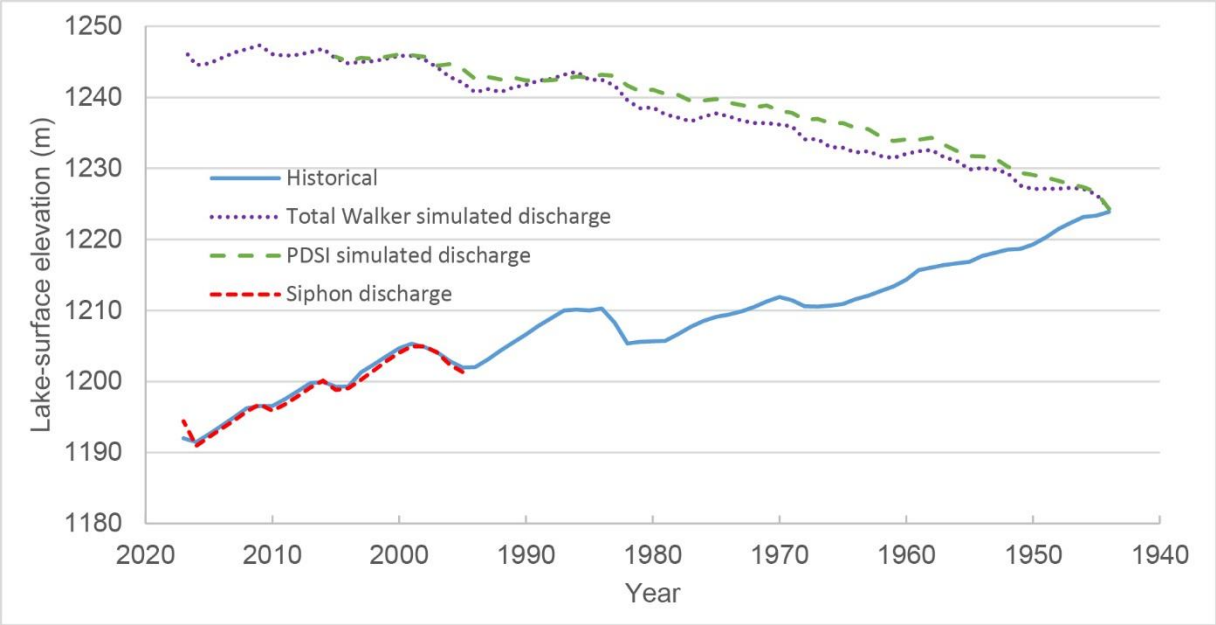
1250
1240
1230
1220
1210
1200
1190
1180
Lake-surface elevation (m)
Historical
Total Walker simulated discharge
PDSI simulated discharge
Siphon discharge
2020
2010
2000
1990
1980
1970
1960
1950
1940
Year

Figure 9

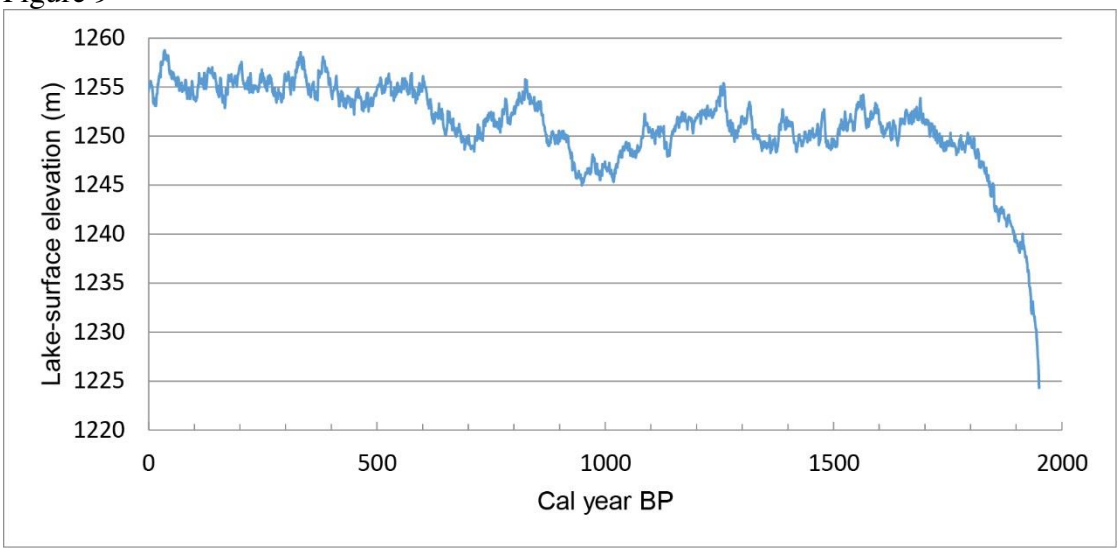
Lake-surface elevation (m)
1260
1255
1250
1245
1240
1235
1230
1225
1220
0
500
1000
1500
2000
Cal year BP

Figure 10

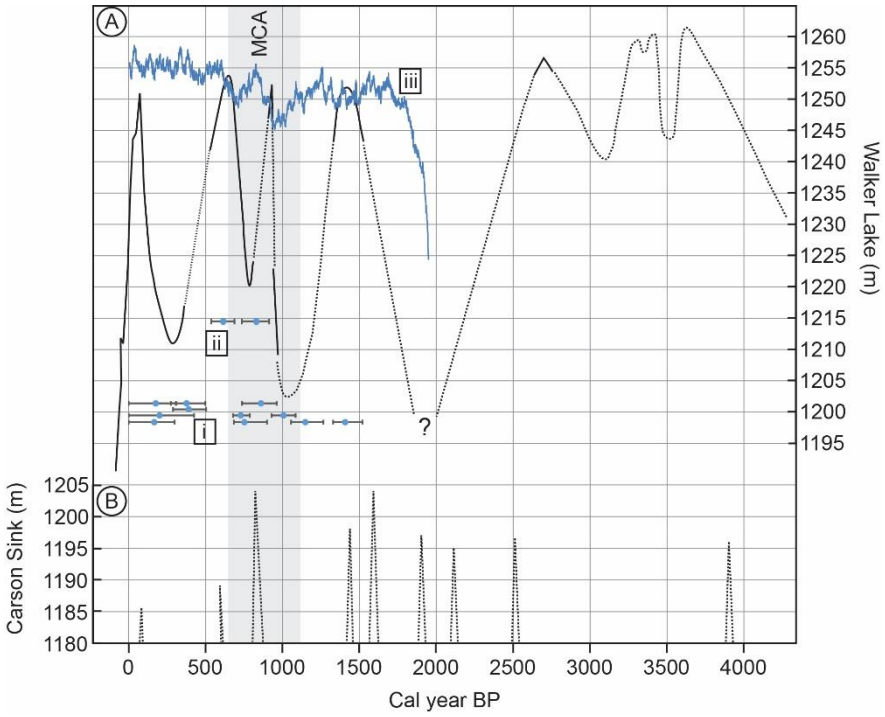
A
MCA
iii
ii
i
?
B
Walker Lake (m)
1260
1255
1250
1245
1240
1235
1230
1225
1220
1215
1210
1205
1200
1195
Carson Sink (m)
1205
1200
1195
1190
1185
1180
0
500
1000
1500
2000
2500
3000
3500
4000
Cal year BP